B850 Ring from Light–Harvesting Complex LH2 - Fluctuations in Dipole Moment Orientations of Bacteriochlorophyll Molecules

Pavel Heřman, David Zapletal

***Abstract*—** Interactions with fluctuated environment strongly influence properties of light–harvesting (LH) pigment–protein complexes. Slow fluctuations could be modeled by static disorder. Several types of these fluctuations are connected with changes of ring geometry. Slow fluctuations of bacteriochlorophyll's dipole moment orientations in B850 ring from LH2 complex of purple bacteria are investigated in present paper. Three modifications of such uncorrelated static disorder type (Gaussian fluctuations of dipole moment orientations in the ring plane, Gaussian fluctuations of dipole moment orientations in a plane which is perpendicular to the ring one and Gaussian fluctuations of dipole moment orientations in arbitrary direction) are taking into account. Distributions of the nearest neighbour transfer integrals are presented and the most important statistical properties are calculated, discussed and compared for different strengths of static disorder.

***Keywords*—**B850 ring, Hamiltonian, LH2 complex, static disorder, transfer integral distributions

I. Introduction

PHOTOSYNTHESIS is the process in which light energy is transformed into chemical energy. This process can take place in different types of organisms, e.g. green plants, bacteria, blue–green algae, etc. The first stage of photosynthesis – light stage – consists of photochemical reactions. Light photon is absorbed in the first stage of photosynthesis (light stage), its energy is used for driving a series of electron transfers and number of photochemical reactions starts. Adenosine triphosphate (ATP) and nicotine adenine dinucleotide phosphate (NADPH – reduced form) are synthesized as the result of this stage. During the second (dark) stage the ATP and NADPH formed in the light–capturing reactions are used for reduction of carbon dioxide to organic carbon compounds [1].

Photosynthesis has been investigated by a lot of researchers for a long time. Our interest is concentrated especially on the first (light) stage of photosynthesis in purple bacteria. Solar photons are absorbed by a complex system of membrane–associated pigment–proteins (light–harvesting (LH) antenna). Then, obtained excitation energy in the form of Frenkel excitons is very effectively transfered to a reaction center. There this energy is converted into a chemical energy [2].

Geometric structures of light–harvesting complexes from purple bacteria are known in great detail from X–ray crystallography. The organization of bacterial light–harvesting complexes is generally the same. Cyclic repetition of identical subunits creates a ring–shaped structure. Various LH complexes (LH1, LH2, LH3, and LH4) can be composed of different number of bacteriochlorophyll molecules and can have different symmetry.

Crystal structure of peripheral light–harvesting complex LH2 contained in purple bacterium *Rhodopseudomonas acidophila* was described by McDermott et al. [3] and then e.g. by Papiz et al. [4]. Bacteriochlorophyll (BChl) molecules in LH2 complex are arranged in two concentric rings (B850 ring and B800 one). B850 ring (with absorption band at about 850 nm) consists of eighteen closely packed BChl molecules and B800 ring contains nine well–separated BChl molecules absorbing around 800 nm. The whole LH2 complex is organized as nonameric system, i.e. it is composed of nine identical subunits. Dipole moments of BChl molecules in LH2 complex are oriented approximately tangentially to the ring. LH2 complexes from other purple bacteria have analogous arrangement.

Some purple bacteria contain also other types of peripheral light–harvesting complexes, e.g. *Rhodopseudomonas acidophila* strain 7050 contains B800–820 LH3 complex and *Rhodopseudomonas palustris* contains LH4 complex. Arrangement of LH3 complex is usually nonameric like LH2 one [5]. LH4 complex is composed of eight identical subunits, i.e. it is octameric, and it consists of three concentric bacteriochlorophyll rings [6]. Additionally, also orientations of BChl dipole moments

Manuscript received June, 2017.

This work was supported by the Faculty of Science, University of Hradec Králové (project of specific research No. 2104/2017 – P. Heřman).

P. Heřman is with the Department of Physics, Faculty of Science, University of Hradec Králové, Rokitanského 62, 50003 Hradec Králové, Czech Republic (e-mail: pavel.herman@uhk.cz).

D. Zapletal is with the Institute of Mathematics and Quantitative Methods, Faculty of Economics and Administration, University of Pardubice, Studentská 95, 53210 Pardubice, Czech Republic (e-mail: david.zapletal@upce.cz).

and consequently strengths of mutual interactions between bacteriochlorophyll molecules can be different in various light–harvesting complexes. For instance, BChl dipole moments in B–α/B–β ring from LH4 complex are oriented approximately radially to the ring. Interactions between the nearest neighbour bacteriochlorophylls in B–α/B–β ring are approximately two times weaker in comparison with B850 ring from LH2 complex and they have opposite sign.

Purple bacteria contain (beside peripheral antenna complexes) also core antenna complexes. For instance LH1 complex from *Rhodopseudomonas acidophila* or *Rhodopseudomonas palustris* consists of approximately 16 structural subunits in which two bacteriochlorophyll molecules are noncovalently attached to pairs of transmembrane polypeptides. These subunits have again ring-like structure which surrounds reaction center [7].

The intermolecular distances of bacteriochlorophyll molecules in LH2 complex are under 1 nm. It implies strong exciton couplings. That is why an extended Frenkel exciton states model can be applied in theoretical approach. The solvent and protein environment of bacteriochlorophyll rings fluctuates. Characteristic time scale of these fluctuations at room temperature has very wide range (from femtoseconds to nanoseconds). Fast fluctuations can be modeled by dynamic disorder (interaction with phonon bath) and slow fluctuations by static disorder. Kumble and Hochstrasser [8] and Nagarajan et al. [9], [10] studied the influence of static disorder in local excitation energies on the anisotropy of fluorescence for LH2 complexes. These investigations were extended by addition of dynamic disorder. This effect was studied by us for simple model systems [11]–[13] and then for models of B850 ring (from LH2) [14], [15]. Also various types of uncorrelated static disorder and correlated one (e.g., elliptical deformation) were considered in our previous investigation [16]–[18]. The results for B850 ring from LH2 complex and B–α/B–β ring from LH4 complex, that have different arrangements of optical dipole moments, were compared in [19]–[22]. Recently, our investigation has been focused on the modeling of absorption and steady state fluorescence spectra of LH2 and LH4 complexes within the nearest neighbour approximation model [23]–[27] and full Hamiltonian model [28]–[36].

Very recently we have started to investigate statistical properties of the nearest neighbour transfer integral distributions for various types of static disorder connected with fluctuations in ring geometry [37]. The results for the fluctuations of BChl molecular positions have been presented in [38]. Main goal of the present paper is the investigation of transfer integral distributions for fluctuations of bacteriochlorophyll dipole moment orientations in B850 ring from LH2 complex. The rest of the paper is structured as follows. Section II introduces the ring model with different types and modifications of static disorder. Used units and parameters could be found in Section III. Results are presented and discussed in Section IV and some conclusions are drawn in Section V.

II. Model

In our model the Hamiltonian of one exciton on molecular ring, e.g. B850 ring from LH2 complex, consists of four terms:

$$H = H^0_{\rm ex} + H_{\rm s} + H_{\rm ph} + H_{\rm ex-ph}. \qquad (1)$$

A. Ideal ring

The first term in Eq. (1),

$$H^0_{\rm ex} = \sum_{m=1}^{N} E^0_m a^\dagger_m a_m + \sum_{m,n=1(m\neq n)}^{N} J^0_{mn} a^\dagger_m a_n, \qquad (2)$$

describes an exciton on the ideal ring, i.e. without any disorder. Here $a^\dagger_m$ (a_m) are creation (annihilation) operators of the exciton at site m, E^0_m is the local excitation energy of m–th molecule, J^0_{mn} (for $m \neq n$) is the so–called transfer integral between sites m and n. N is the number of molecules in the ring ($N = 18$ for B850 ring from LH2 complex). Local excitation energies E^0_m are the same for all bacteriochlorophylls on unperturbed ring, i.e.

$$E^0_m = E_0, \quad m = 1, \ldots, N.$$

The interaction strengths between the nearest neighbour bacteriochlorophylls inside one subunit and between subunits are almost the same in B850 ring from LH2 complex (see Figure 1 (B) in [6]). That is why such ring can be modeled as homogeneous case,

$$J^0_{mn} = J^0_{m+i,n+i}. \qquad (3)$$

Transfer integrals J_{mn} in dipole–dipole approximation read

$$J_{mn} = \frac{\vec{d}_m \cdot \vec{d}_n}{|\vec{r}_{mn}|^3} - 3\frac{\left(\vec{d}_m \cdot \vec{r}_{mn}\right)\left(\vec{d}_n \cdot \vec{r}_{mn}\right)}{|\vec{r}_{mn}|^5} =$$

$$= |\vec{d}_m||\vec{d}_n|\frac{\cos\varphi_{mn} - 3\cos\varphi_m \cos\varphi_n}{|\vec{r}_{mn}|^3}. \qquad (4)$$

Local dipole moments of m–th and n–th molecule are denoted as $\vec{d}_m$ and $\vec{d}_n$, the angle between these dipole moment vectors ($\vec{d}_m$, $\vec{d}_n$) is referred to as φ_{mn}. $\vec{r}_{mn}$ represents the vector connecting m–th and n–th molecule, φ_m (φ_n) symbolizes the angle between $\vec{d}_m$ ($\vec{d}_n$) and $\vec{r}_{mn}$. In case of ideal ring (without any disorder) we consider the same distances $r_{m,m+1}$ of neighbouring bacteriochlorophyll molecules. Therefore angles $\beta_{m,m+1}$ have to be the same too ($\beta_{m,m+1} = 2\pi/18$, see Figure 1). The reason for this is the requirement of correspondence between the geometric arrangement of B850 ring and

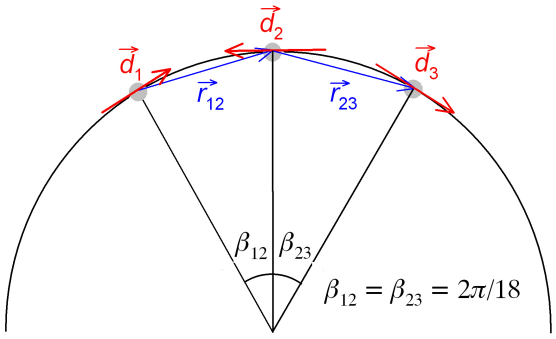

Fig. 1. Geometric arrangement of ideal B850 ring from LH2 complex (without any fluctuations – dipole moments are oriented tangentially to the ring)

interaction strengths between the nearest neighbour bacteriochlorophylls.

In what follows we consider that only the nearest neighbour transfer matrix elements are nonzero, i.e. the nearest neighbour approximation model. In this case we have

$$J^0_{mn} = J_0(\delta_{m,n+1} + \delta_{m,n-1}). \tag{5}$$

The wave vector representation with corresponding delocalized Bloch states α and energies E_α can be used for diagonalization of the pure exciton Hamiltonian $H^0_{\rm ex}$. Then $H^0_{\rm ex}$ reads

$$H^0_{\rm ex} = \sum_{\alpha=1}^{N} E_\alpha a^\dagger_\alpha a_\alpha, \tag{6}$$

with a_α (Fourier transformed excitonic operator in α–representation). Considering homogeneous case and the nearest neighbour approximation model, the operators a_α and the energies E_α from Eq. (6) have the form

$$a_\alpha = \sum_{n=1}^{N} a_n e^{i\alpha n},\ \alpha = \frac{2\pi}{N} l,\ l = 0, \ldots, \pm\frac{N}{2}, \tag{7}$$

$$E_\alpha = E_0 - 2J_0 \cos\alpha. \tag{8}$$

B. Static disorder

The second term in Eq. 1, $H_{\rm s}$, corresponds to static disorder. One of the ways to take into account such disorder is to model it as slow fluctuations in ring geometry. Deviation in ring geometry results in changes of transfer integrals δJ_{mn} $(m \neq n)$,

$$J_{mn} = J_{nm} = J^0_{mn} + \delta J_{mn}. \tag{9}$$

Static disorder in ring geometry can be consider in two ways – fluctuations in molecular positions or fluctuations in molecular dipole moment orientations. We studied first type of fluctuations as only in the ideal ring plane [37] as out of the ideal ring plane [38]. In the present paper we investigate the second type, i.e. deviations of molecular dipole moment orientations.

The simplest possibility is to neglect the changes of dipole moment orientations out of the ring plane. Then we have:

a) uncorrelated fluctuations of molecular dipole moment orientations $\delta\theta_m$ in the plane of ideal ring (Gaussian distribution and standard deviation Δ_θ),

$$\theta_m = \theta^0_m + \delta\theta_m, \tag{10}$$

where θ^0_m characterizes the dipole moment direction of m–the molecule in the ideal ring (see Figure 2).

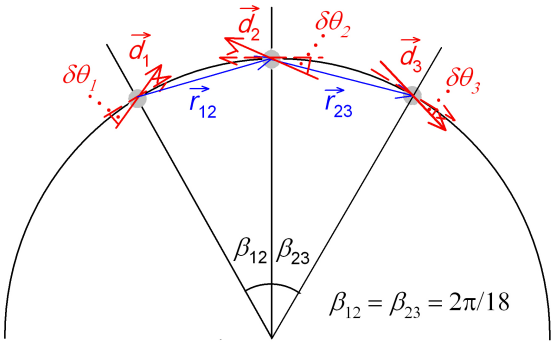

Fig. 2. B850 ring from LH2 complex – fluctuations in bacteriochlorophyll dipole moment orientations $\delta\theta_m$ in the ideal ring plane

If the dipole moment orientations are changed out of the ideal ring plane, we get:

b) uncorrelated fluctuations of molecular dipole moment orientations $\delta\gamma_m$ – fluctuations occur only in the plane which is perpendicular to the ideal ring one (Gaussian distribution and standard deviation Δ_γ),

$$\gamma_m = \delta\gamma_m. \tag{11}$$

Here γ_m determines the angle between m–th dipole moment vector and the plane of the ideal ring. (see Figure 3).

Previous two types are included in more general type of geometric disorder:

c) uncorrelated fluctuations of bacteriochlorophyll dipole moment orientations in arbitrary direction $\delta\psi_m$,

$$\psi_m = \delta\psi_m.$$

Here ψ_m denotes the angle between m–th dipole moment vector (in disordered ring) and the vector of m–th dipole moment in the ideal ring. The distributions of the angles $\delta\psi_m$ are supposed to be uncorrelated with Gaussian distribution and standard deviation Δ_ψ. Distributions of angles φ_m are supposed to be uncorrelated and uniform (see Figure 4).

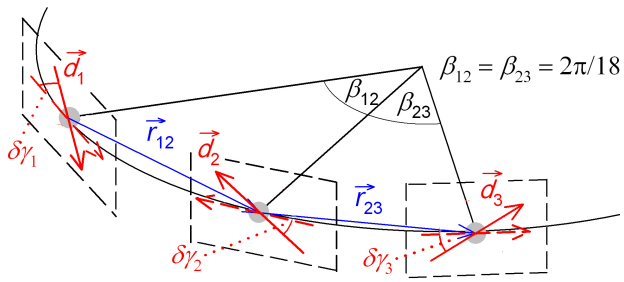

Fig. 3. B850 ring from LH2 complex – fluctuations in bacteriochlorophyll dipole moment orientations $\delta\gamma_m$ in the plane which is perpendicular to the ideal ring one

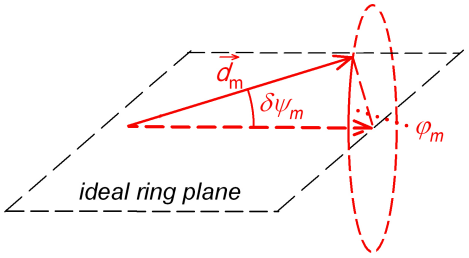

Fig. 4. B850 ring from LH2 complex – fluctuations in bacteriochlorophyll dipole moment orientations $\delta\psi_m$ in arbitrary direction

Due to the consideration of dipole–dipole approximation the connection between disorder in geometric arrangement and in transfer integrals is given by Eq. (4).

C. Dynamic disorder

Finally, the third and fourth term in Eq (1),

$$H_{\mathrm{ph}} = \sum_q \hbar\omega_q b_q^\dagger b_q, \tag{12}$$

$$H_{\mathrm{ex-ph}} = \frac{1}{\sqrt{N}} \sum_m \sum_q G_q^m \hbar\omega_q a_m^\dagger a_m (b_q^\dagger + b_q), \tag{13}$$

represents dynamic disorder, i.e. phonon bath in the harmonic approximation and exciton–phonon interaction. The phonon creation and annihilation operators are denoted by $b_q^\dagger$ and b_q, respectively, and G_q^m denotes the exciton-phonon coupling constant. In this paper the distributions of transfer integrals are investigated and therefore these terms can be neglected.

III. Units and Parameters

Dimensionless energies normalized to the transfer integral $J_{m,m+1} = J_0$ (see Eq. (5)) have been used in our calculations. Estimation of J_0 varies in literature between 250 cm^{-1} and 400 cm^{-1}.

In our previous investigations [39] we found from comparison with experimental results for B850 ring from the LH2 complex [40] that the possible strength Δ_J of the uncorrelated Gaussian static disorder in transfer integrals δJ_{mn} is approximately $\Delta_J \approx 0.15\ J_0$. The strengths of above mentioned types of static disorder in ring geometry is taken in connection with the strength Δ_J. That is why for our types of static disorder we have taken the strengths in following intervals:

a) uncorrelated fluctuations of molecular dipole moment orientations $\delta\theta_m$ in the plane of ideal ring

$$\Delta_\theta \in \langle 0.02\ \pi, 0.20\ \pi \rangle,$$

b) uncorrelated fluctuations of molecular dipole moment orientations $\delta\gamma_m$ only in the plane which is perpendicular to the ideal ring one

$$\Delta_\gamma \in \langle 0.02\ \pi, 0.20\ \pi \rangle,$$

c) uncorrelated fluctuations of bacteriochlorophyll dipole moment orientations $\delta\psi_m$ in arbitrary direction

$$\Delta_\psi \in \langle 0.02\ \pi, 0.20\ \pi \rangle.$$

In all cases calculations were done for 10000 realizations of static disorder.

IV. Results and Discussion

Hamiltonian of B850 ring from LH2 complex is strongly influenced by static disorder in ring geometry. In this paper we are dealing with one type of such fluctuations, namely fluctuations in molecular dipole moment orientations. Calculated distributions of the nearest neighbour transfer integrals $J_{m,m+1}$ are shown and compared for three above mentioned modifications of such static disorder type. Graphical presentation of these distributions is done by contour plots and by line plots. Values of $E(J_{m,m+1})$ and $E(J_{m,m+1}) \pm \sqrt{D(J_{m,m+1})}$ are also included in contour plots. Here $E(J_{m,m+1})$ is sample expected value and $\sqrt{D(J_{m,m+1})}$ is sample standard deviation,

$$E(J_{m,m+1}) = \frac{1}{n} \sum_{i=1}^{n} J_{m,m+1}, \tag{14}$$

$$\sqrt{D(J_{m,m+1})} = \sqrt{\frac{1}{(n-1)} M_2}. \tag{15}$$

In addition, sample skewness α_3,

$$\alpha_3 = \frac{n^{\frac{5}{2}}}{(n-1)(n-2)} \frac{M_3}{M_2^{\frac{3}{2}}}, \tag{16}$$

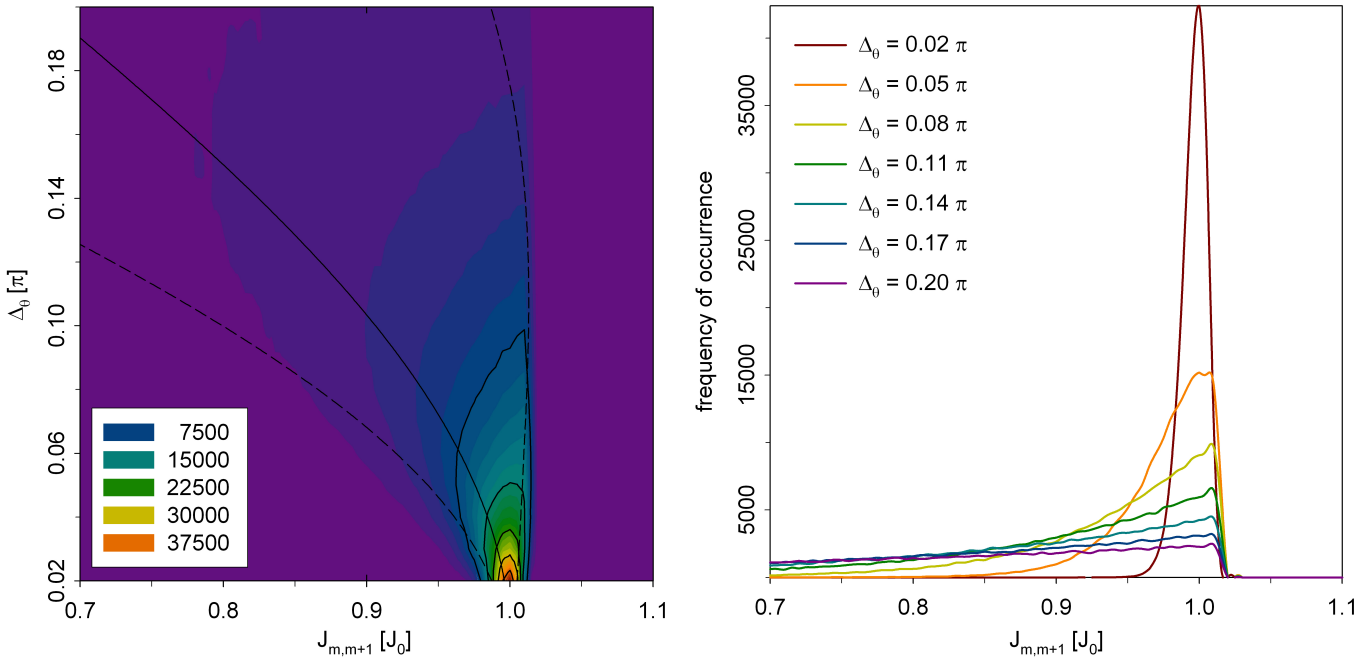

Fig. 5. Distributions of the nearest neighbour transfer integrals $J_{m,m+1}$ for B850 ring from LH2 complex – uncorrelated Gaussian fluctuations $\delta\theta_m$ in molecular dipole moment directions in the plane of ideal ring; standard deviation (the strength of static disorder) $\Delta_\theta \in \langle 0.02\ \pi, 0.20\ \pi\rangle$; left column – contour plot with the dependencies of $E(J_{m,m+1})$ (solid line) and $E(J_{m,m+1}) \pm \sqrt{D(J_{m,m+1})}$ (dashed lines) on Δ_θ, right column – line plots for chosen values of Δ_θ

Δ_θ	expected value $E(J_{m,m+1})$	standard deviation $\sqrt{D(J_{m,m+1})}$	skewness α_3	kurtosis α_4	coefficient of variation c
0.02 π	0.996 J_0	0.009 J_0	-0.787	0.999	0.009
0.05 π	0.976 J_0	0.033 J_0	-1.684	4.613	0.034
0.08 π	0.939 J_0	0.073 J_0	-1.954	5.827	0.078
0.11 π	0.888 J_0	0.126 J_0	-1.941	5.353	0.141
0.14 π	0.824 J_0	0.186 J_0	-1.811	4.261	0.226
0.17 π	0.752 J_0	0.250 J_0	-1.629	3.057	0.332
0.20 π	0.674 J_0	0.312 J_0	-1.428	1.965	0.463

TABLE I

EXPECTED VALUE, STANDARD DEVIATION, SKEWNESS, KURTOSIS AND COEFFICIENT OF VARIATION FOR THE NEAREST NEIGHBOUR TRANSFER INTEGRAL $J_{m,m+1}$ DISTRIBUTIONS OF UNCORRELATED GAUSSIAN FLUCTUATIONS OF MOLECULAR DIPOLE MOMENT ORIENTATIONS $\delta\theta_m$ IN THE PLANE OF IDEAL RING (SEVEN STRENGTHS Δ_θ)

and sample kurtosis α_4,

$$\alpha_4 = \frac{n^2}{(n-2)(n-3)}\left[\frac{n(n+1)}{n-1}\frac{M_4}{M_2^2} - 3\right], \qquad (17)$$

are calculated. Here M_k denotes k–th central moment of $J_{m,m+1}$,

$$M_k = \sum_{i=1}^{n}\left[J_{m,m+1} - E(J_{m,m+1})\right]^k, \qquad (18)$$

and n is the number of cases in our samples. Different modifications of static disorder in molecular dipole moment orientations are compared in detail by sample coefficient of variation c:

$$c = \frac{\sqrt{D(J_{m,m+1})}}{E(J_{m,m+1})}. \qquad (19)$$

Because B850 ring from LH2 complex contains 18 bacteriochlorophylls, the dimension of our Hamilto-

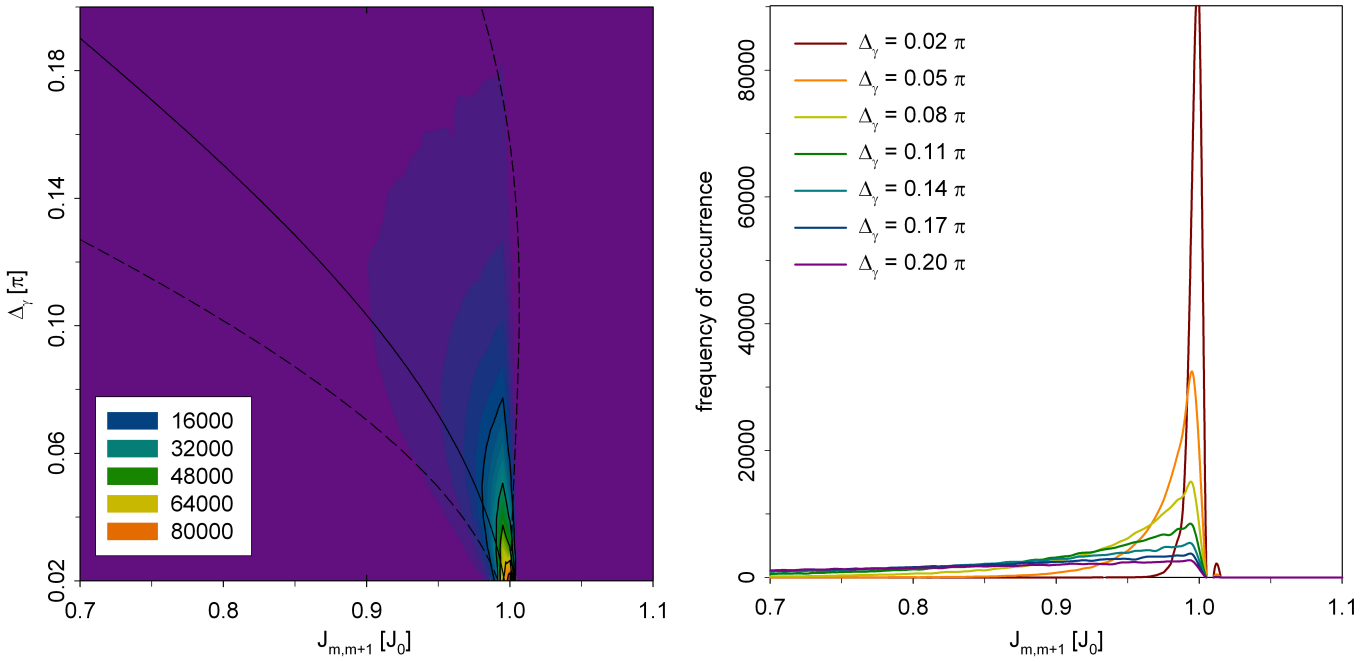

Fig. 6. Distributions of the nearest neighbour transfer integrals $J_{m,m+1}$ for B850 ring from LH2 complex – uncorrelated Gaussian fluctuations $\delta\gamma_m$ of molecular dipole moment orientations only in the plane which is perpendicular to the ideal ring one; standard deviation (the strength of static disorder) $\Delta_\gamma \in \langle 0.02\ \pi, 0.20\ \pi\rangle$; left column – contour plot with the dependencies of $E(J_{m,m+1})$ (solid line) and $E(J_{m,m+1}) \pm \sqrt{D(J_{m,m+1})}$ (dashed lines) on Δ_γ, right column – line plots for chosen values of Δ_γ

Δ_γ	expected value $E(J_{m,m+1})$	standard deviation $\sqrt{D(J_{m,m+1})}$	skewness α_3	kurtosis α_4	coefficient of variation c
0.02 π	0.996 J_0	0.004 J_0	-2.493	9.610	0.004
0.05 π	0.976 J_0	0.027 J_0	-2.419	8.879	0.028
0.08 π	0.939 J_0	0.066 J_0	-2.288	7.666	0.071
0.11 π	0.888 J_0	0.119 J_0	-2.113	6.182	0.134
0.14 π	0.824 J_0	0.180 J_0	-1.907	4.646	0.218
0.17 π	0.752 J_0	0.244 J_0	-1.685	3.231	0.324
0.20 π	0.674 J_0	0.306 J_0	-1.462	2.034	0.454

TABLE II

EXPECTED VALUE, STANDARD DEVIATION, SKEWNESS, KURTOSIS AND COEFFICIENT OF VARIATION FOR THE NEAREST NEIGHBOUR TRANSFER INTEGRAL $J_{m,m+1}$ DISTRIBUTIONS OF UNCORRELATED GAUSSIAN FLUCTUATIONS $\delta\gamma_m$ OF MOLECULAR DIPOLE MOMENT ORIENTATIONS ONLY IN THE PLANE WHICH IS PERPENDICULAR TO THE IDEAL RING ONE (SEVEN STRENGTHS Δ_γ)

nian $N = 18$. Our results were calculated from 10000 realizations of static disorder and then the number of cases n in our samples equals 180000.

Distributions of the nearest neighbour transfer integrals $J_{m,m+1}$ for above mentioned types of static disorder are presented in Figure 5 – Figure 7. Distributions of $J_{m,m+1}$ for Gaussian uncorrelated fluctuations $\delta\theta_m$ of molecular dipole moment orientations in the plane of ideal ring are drawn in Figure 5. Figure 6 and Figure 7 show the distributions of $J_{m,m+1}$ for other two above mentioned types of static disorder (Gaussian uncorrelated fluctuations $\delta\gamma_m$ of molecular dipole moment orientations in the plane which is perpendicular to the ideal ring one and Gaussian uncorrelated fluctuations $\delta\psi_m$ of molecular dipole moment orientations in arbitrary direction).

Dependencies of sample expected value $E(J_{m,m+1})$ and sample standard deviation $\sqrt{D(J_{m,m+1})}$ on corresponding static disorder strength are also pre-

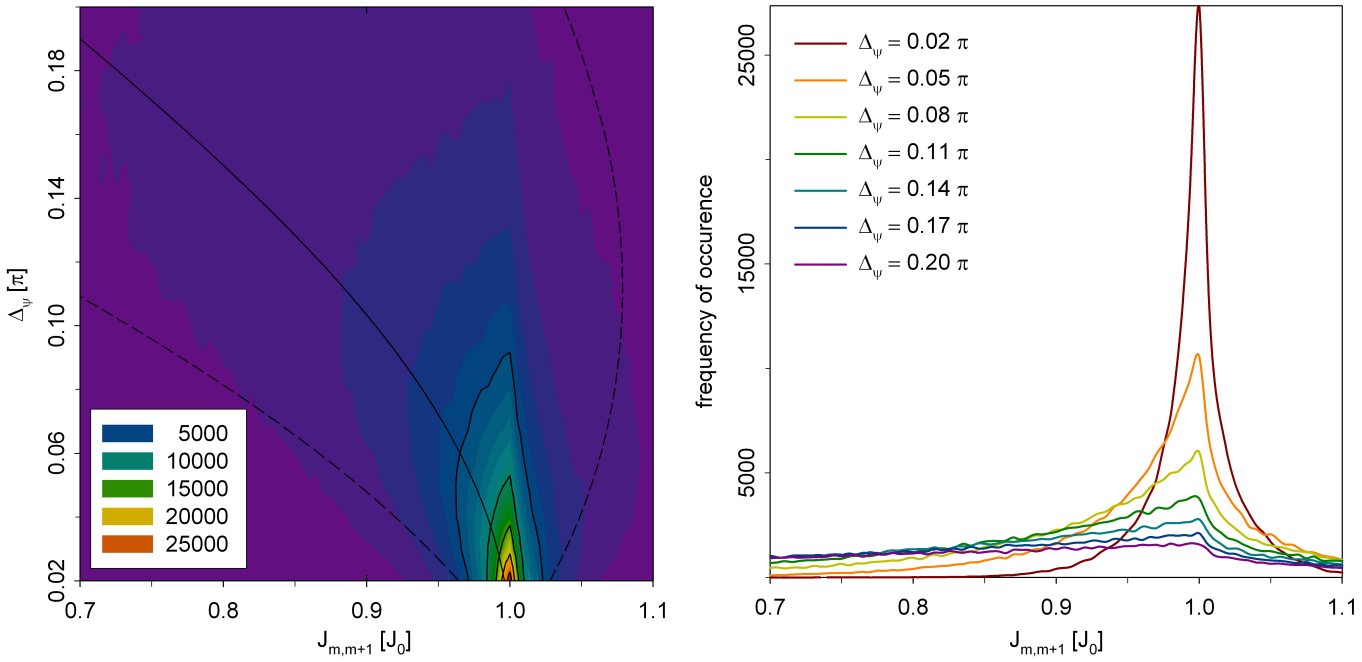

Fig. 7. Distributions of the nearest neighbour transfer integrals $J_{m,m+1}$ for B850 ring from LH2 complex – uncorrelated Gaussian fluctuations $\delta\psi_m$ of dipole bacteriochlorophyll orientations in arbitrary direction; standard deviation (the strength of static disorder) $\Delta_\psi \in \langle 0.02\ \pi, 0.20\ \pi \rangle$; left column – contour plot with the dependencies of $E(J_{m,m+1})$ (solid line) and $E(J_{m,m+1}) \pm \sqrt{D(J_{m,m+1})}$ (dashed lines) on Δ_ψ, right column – line plots for chosen values of Δ_ψ

Δ_ψ	expected value $E(J_{m,m+1})$	standard deviation $\sqrt{D(J_{m,m+1})}$	skewness α_3	kurtosis α_4	coefficient of variation c
0.02 π	0.996 J_0	0.032 J_0	-0.364	3.565	0.032
0.05 π	0.976 J_0	0.081 J_0	-0.821	3.621	0.083
0.08 π	0.939 J_0	0.134 J_0	-1.110	3.502	0.143
0.11 π	0.887 J_0	0.191 J_0	-1.235	3.103	0.215
0.14 π	0.824 J_0	0.250 J_0	-1.238	2.499	0.303
0.17 π	0.752 J_0	0.309 J_0	-1.165	1.830	0.411
0.20 π	0.674 J_0	0.364 J_0	-1.053	1.200	0.541

TABLE III

EXPECTED VALUE, STANDARD DEVIATION, SKEWNESS, KURTOSIS AND COEFFICIENT OF VARIATION FOR THE NEAREST NEIGHBOUR TRANSFER INTEGRAL $J_{m,m+1}$ DISTRIBUTIONS FOR UNCORRELATED FLUCTUATIONS OF BACTERIOCHLOROPHYLL DIPOLE MOMENT ORIENTATIONS $\delta\psi_m$ IN ARBITRARY DIRECTION (SEVEN STRENGTHS Δ_ψ)

sented in contour plots ($E(J_{m,m+1})$: solid line, $E(J_{m,m+1}) \pm \sqrt{D(J_{m,m+1})}$: dashed lines). Additionally, Table I – Table III contain the values of sample characteristics $E(J_{m,m+1})$, $\sqrt{D(J_{m,m+1})}$, α_3, α_4 and c (see Eq. (14) – Eq. (19)) for chosen static disorder strengths. The distributions of $J_{m,m+1}$ are also presented as line plots for the same strengths of static disorder in Figure 5 – left column ($\delta\theta_m$), Figure 5 – right column, Figure 6 – right column ($\delta\gamma_m$) and Figure 7 – right column ($\delta\psi_m$).

At the present paper we focus only on the types of static disorder connected with deviations in molecular dipole moment orientations ($\delta\theta_m$, $\delta\gamma_m$ and $\delta\psi_m$). If we consider Gaussian distributions of $\delta\theta_m$, $\delta\gamma_m$ and $\delta\psi_m$, resulting distributions of the nearest neighbour transfer integrals $J_{m,m+1}$ are non–Gaussian. It is clear (from Figures 5 – 7 and Tables I – III) that the expected value $E(J_{m,m+1})$ is non–constant and standard deviation

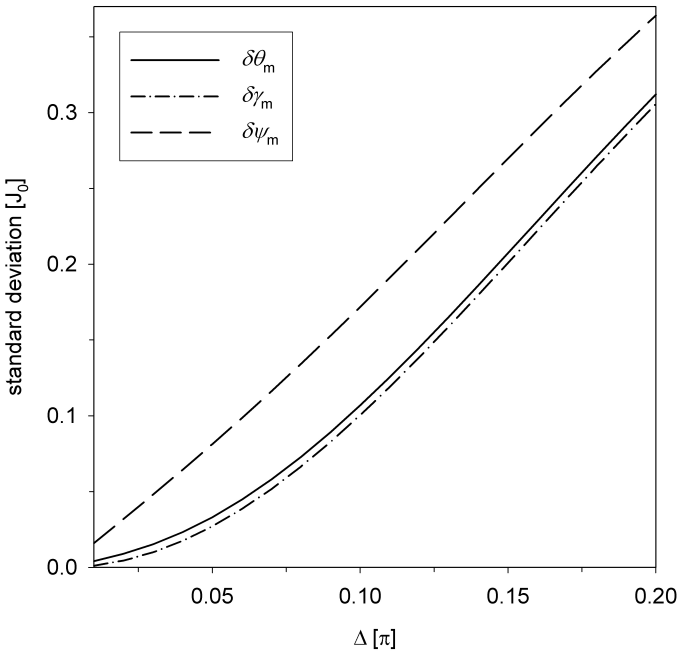

Fig. 8. Dependence of standard deviations $\sqrt{D(J_{m,m+1})}$ on static disorder strength Δ for three types of Gaussian uncorrelated fluctuations $\delta\theta_m$, $\delta\gamma_m$ and $\delta\psi_m$

$\sqrt{D(J_{m,m+1})}$ depends on static disorder strength for all these three static disorder types. On the other hand, Gaussian distribution of transfer integrals $J_{m,m+1}$ has constant expected value, i.e. $E(J_{m,m+1}) = J_0$, and standard deviation equals the strength of static disorder $\sqrt{D(J_{m,m+1})} = \Delta_J$. Level of deviation from Gaussian distribution can also be assessed through skewness α_3 and kurtosis α_4. These characteristics are nonconstant for all three static disorder types connected with fluctuations in molecular dipole moment orientations (contrary, $\alpha_3 = \alpha_4 = 0$ for Gaussian distribution). As concerns expected value $E(J_{m,m+1})$, we can see decrease of this characteristics for increasing static disorder strength in all three cases of fluctuations ($\delta\theta_m$, $\delta\gamma_m$ and $\delta\psi_m$). Values of $E(J_{m,m+1})$ are practically the same for all three types of static disorder. The dependencies of standard deviation $\sqrt{D(J_{m,m+1})}$ on static disorder strength are very similar in case of $\delta\theta_m$ and $\delta\gamma_m$. They are nonlinear for small static disorder strengths ($\Delta \in \langle 0.02\ \pi, 0.10\ \pi\rangle$) and they become approximately linear for higher values of Δ. On the other hand, the dependence of standard deviation $\sqrt{D(J_{m,m+1})}$ on static disorder strength is different from previous two ones in case of the third type of static disorder ($\delta\psi_m$). It is approximately linear in whole interval of Δ ($\Delta \in \langle 0.02\ \pi, 0.20\ \pi\rangle$)) and the values of $\sqrt{D(J_{m,m+1})}$ are higher in comparison with previous two types (see Table I – III and Figure 8).

The distributions of $J_{m,m+1}$ are negatively skewed (to the left hand side) for all three static disorder types (see Figure 5 – Figure 7, right columns). It corresponds with negative values of sample skewness (see Table I – III). All these distributions have also higher sample kurtosis α_4 in comparison with Gaussian distribution of $J_{m,m+1}$ ($\alpha_4 = 0$ for this distribution). The dependencies of the kurtosis α_4 have their maximum approximately in the middle of our interval of Δ in case of static disorder $\delta\theta_m$ and $\delta\psi_m$. Contrary, the dependence of α_4 on Δ is monotonous for static disorder $\delta\gamma_m$. In this case the value of α_4 is highest for the lowest value of Δ and vice versa.

Due to nonconstant expected value, influences of different types of fluctuations to distribution of $J_{m,m+1}$ can be compared using the coefficient of variation c. Our previous investigations [39] led to suitable strength of static disorder in transfer integrals $\Delta_J \approx 0.15\ J_0$ and consequently $c \approx 0.15$. As concerns fluctuations in molecular dipole moment orientations, approximately same value of the coefficient of variation c corresponds to the following disorder strengths: $\Delta_\theta \approx 0.11 - 0.12\ \pi$, $\Delta_\gamma \approx 0.12\pi$ and $\Delta_\psi \approx 0.08 - 0.09\ \pi$.

V. Conclusions

Summarization of the results obtained within different types of static disorder connected with fluctuations in molecular dipole moment orientations and their comparison can be done as follows. Expected value of the nearest neighbour transfer integral distribution depends on static disorder strength. The dependences are practically the same for all three presented types of fluctuations. The dependence of standard deviation of the nearest neighbour transfer integral distribution on the static disorder strength shows the nonlinearity in case of fluctuations in molecular dipole moment directions in the plane of ideal ring $\delta\theta_m$ and also in case of fluctuations in molecular dipole moment directions in the plane which is perpendicular to the ideal ring one $\delta\gamma_m$. For all three types of static disorder in molecular dipole moment orientations the distributions of $J_{m,m+1}$ are significantly skewed and have nonzero kurtosis. The comparison of coefficient of variation c allows us to estimate suitable strength of static disorder for dofferent static disorder types.

References

[1] D. W. Lawlor, *Photosynthesis*, Spriger, New York 2001.
[2] R. van Grondelle and V. I. Novoderezhkin, Energy transfer in photosynthesis: experimental insights and quantitative models, *Phys. Chem. Chem. Phys.* 8, 2003, pp. 793–807.
[3] G. McDermott, et al., Crystal structure of an integral membrane light-harvesting complex from photosynthetic bacteria, *Nature* 374, 1995, pp. 517–521.
[4] M. Z. Papiz, et al., The structure and thermal motion of the B 800-B850 LH2 complex from Rps. acidophila at 2.0 A resolution and 100 K: new structural features and functionally relevant motions, *J. Mol. Biol.* 326, 2003, pp. 1523–1538.

[5] K. McLuskey, et al., The crystalographic structure of the B800–820 LH3 light-harvesting complex from the purple bacteria Rhodopseudomonas acidophila strain 7050, *Biochemistry* 40, 2001, pp. 8783–8789.

[6] W. P. F. de Ruijter, et al., Observation of the Energy–Level Structure of the Low–Light Adapted B800 LH4 Complex by Single–Molecule Spectroscopy, *Biophys. J.* 87, 2004, pp. 3413–3420.

[7] A. W. Roszak, et al., Crystal structure of the RC-LH1 core complex from Rhodopseudomonas palustris, *Science* 302, 2003, pp. 1976–1972.

[8] R. Kumble and R. Hochstrasser, Disorder–induced exciton scattering in the light–harvesting systems of purple bacteria: Influence on the anisotropy of emission and band $\rightarrow$ band transitions, *J. Chem. Phys.* 109, 1998, pp. 855–865.

[9] V. Nagarajan, et al., Femtosecond pump–probe spectroscopy of the B850 antenna complex of Rhodobacter sphaeroides at room temperature, *J. Phys. Chem. B* 103, 1999, pp. 2297–2309.

[10] V. Nagarajan and W. W. Parson, Femtosecond fluorescence depletion anisotropy: Application to the B850 antenna complex of Rhodobacter sphaeroides, *J. Phys. Chem. B* 104, 2000, pp. 4010–4013.

[11] V. Čápek, I. Barvík and P. Heřman, Towards proper parametrization in the exciton transfer and relaxation problem: dimer, *Chem. Phys.* 270, 2001, pp. 141–156.

[12] P. Heřman and I. Barvík, Towards proper parametrization in the exciton transfer and relaxation problem. II. Trimer, *Chem. Phys.* 274, 2001, pp. 199–217.

[13] P. Heřman, I. Barvík and M. Urbanec, Energy relaxation and transfer in excitonic trimer, *J. Lumin.* 108, 2004, pp. 85–89.

[14] P. Heřman, et al., Exciton scattering in light–harvesting systems of purple bacteria, *J. Lumin.* 94–95, 2001, pp. 447–450.

[15] P. Heřman and I. Barvík, Non–Markovian effects in the anisotropy of emission in the ring antenna subunits of purple bacteria photosynthetic systems, *Czech. J. Phys.* 53, 2003, pp. 579–605.

[16] P. Heřman, et al., Influence of static and dynamic disorder on the anisotropy of emission in the ring antenna subunits of purple bacteria photosynthetic systems, *Chem. Phys.* 275, 2002, pp. 1–13.

[17] P. Heřman and I. Barvík, Temperature dependence of the anisotropy of fluorescence in ring molecular systems, *J. Lumin.* 122–123, 2007, pp. 558–561.

[18] P. Heřman, D. Zapletal and I. Barvík, Computer simulation of the anisotropy of fluorescence in ring molecular systems: Influence of disorder and ellipticity, *Proc. IEEE 12th Int. Conf. on Computational Science and Engineering*, Vancouver: IEEE Comp. Soc., 2009, pp. 437–442.

[19] P. Heřman and I. Barvík, Coherence effects in ring molecular systems, *Phys. Stat. Sol. C* 3, 2006, 3408–3413.

[20] P. Heřman, D. Zapletal and I. Barvík, The anisotropy of fluorescence in ring units III: Tangential versus radial dipole arrangement, *J. Lumin.* 128, 2008, pp. 768–770.

[21] P. Heřman, I. Barvík and D. Zapletal, Computer simulation of the anisotropy of fluorescence in ring molecular systems: Tangential vs. radial dipole arrangement, *Lecture Notes in Computer Science* 5101, 2008, pp. 661–670.

[22] P. Heřman, D. Zapletal and I. Barvík, Lost of coherence due to disorder in molecular rings, *Phys. Stat. Sol. C* 6, 2009, pp. 89–92.

[23] P. Heřman, D. Zapletal and J. Šlégr, Comparison of emission spectra of single LH2 complex for different types of disorder, *Phys. Proc.* 13, 2011, pp. 14–17.

[24] D. Zapletal and P. Heřman, Simulation of molecular ring emission spectra: localization of exciton states and dynamics, *Int. J. Math. Comp. Sim.* 6, 2012, pp. 144–152.

[25] M. Horák, P. Heřman and D. Zapletal, Simulation of molecular ring emission spectra – LH4 complex: localization of exciton states and dynamics, *Int. J. Math. Comp. Sim.* 7, 2013, pp. 85–93.

[26] P. Heřman and D. Zapletal, Intermolecular coupling fluctuation effect on absorption and emission spectra for LH4 ring, *Int. J. Math. Comp. Sim.* 7, 2013, pp. 249–257.

[27] M. Horák, P. Heřman and D. Zapletal, Modeling of emission spectra for molecular rings – LH2, LH4 complexes, *Phys. Proc.* 44, 2013, pp. 10–18.

[28] P. Heřman, D. Zapletal and M. Horák, Emission spectra of LH2 complex: full Hamiltonian model, *Eur. Phys. J. B* 86, 2013, art. no. 215.

[29] P. Heřman and D. Zapletal, Emission Spectra of LH4 Complex: Full Hamiltonian Model, *Int. J. Math. Comp. Sim.* 7, 2013, pp. 448–455.

[30] P. Heřman and D. Zapletal, Simulation of Emission Spectra for LH4 Ring: Intermolecular Coupling Fluctuation Effect, *Int. J. Math. Comp. Sim.* 8, 2014, pp. 73–81.

[31] D. Zapletal and P. Heřman, Photosynthetic complex LH2 – Absorption and steady state fluorescence spectra, *Energy* 77, 2014, pp. 212–219.

[32] P. Heřman and D. Zapletal, Simulations of emission spectra for LH4 Ring – Fluctuations in radial positions of molecules, *Int. J. Biol. Biomed. Eng.* 9, 2015, pp. 65–74.

[33] P. Heřman and D. Zapletal, Computer simulation of emission and absorption spectra for LH2 ring, *LNEE* 343, 2015, pp. 221–234.

[34] P. Heřman and D. Zapletal, Modeling of Absorption and Steady State Fluorescence Spectra of Full LH2 Complex (B850 – B800 Ring), *Int. J. Math. Mod. Meth. Appl. Sci.* 9, 2015, pp. 614–623.

[35] P. Heřman and D. Zapletal, Modeling of Emission and Absorption Spectra of LH2 Complex (B850 and B800 Ring) – Full Hamiltonian Model, *Int. J. Math. Comp. Sim.* 10, 2016, pp. 208–217.

[36] P. Heřman and D. Zapletal, B–α/B–β Ring from Photosynthetic Complex LH4, Modeling of Absorption and Fluorescence Spectra, *Int. J. Math. Comp. Sim.* 10, 2016, pp. 332–344.

[37] P. Heřman and D. Zapletal, B850 Ring from Photosynthetic Complex LH2 - Comparison of Different Static Disorder Types, *Int. J. Math. Comp. Sim.* 10, 2016, pp. 361–369.

[38] P. Heřman and D. Zapletal, Fluctuations of Bacteriochlorophylls Positions in B850 Ring from Photosynthetic Complex LH2 *Int. J. Math. Comp. Sim.* 10, 2016, pp. 381–389.

[39] P. Heřman, I. Barvík and D. Zapletal, Energetic disorder and exciton states of individual molecular rings, *J. Lumin.* 119–120, 2006, pp. 496–503.

[40] C. Hofmann, T. J. Aartsma and J. Kőhler, Energetic disorder and the B850–exciton states of individual light–harvesting 2 complexes from Rhodopseudomonas acidophila, *Chem. Phys. Lett.* 395, 2004, pp. 373–378.